



# Source-Reservoir Characteristics and Accumulation of Gas Chimney-Type Gas Hydrates in Qiongdongnan Basin, Northern South China Sea

Qi Fan<sup>1,2\*</sup>, Qingping Li<sup>1,2</sup>, Shouwei Zhou<sup>2,3</sup>, Lixia Li<sup>1,2</sup>, Zhenyu Zhu<sup>1,2</sup> and Xin Lv<sup>1,2</sup>

<sup>1</sup>CNOOC Research Institute Company Limited, Beijing, China, <sup>2</sup>State Key Laboratory of Natural Gas Hydrates, Beijing, China, <sup>3</sup>China National Offshore Oil Company, Beijing, China

## OPEN ACCESS

### Edited by:

Pibo Su,  
Guangzhou Marine Geological Survey,  
China

### Reviewed by:

Zhifeng Wan,  
Sun Yat-sen University, China  
Qing Li,  
Qingdao Institute of Marine Geology  
(QIMG), China

### \*Correspondence:

Qi Fan  
fanqi@cnooc.com.cn

### Specialty section:

This article was submitted to  
Sedimentology, Stratigraphy and  
Diagenesis,  
a section of the journal  
Frontiers in Earth Science

Received: 21 February 2022

Accepted: 01 April 2022

Published: 25 April 2022

### Citation:

Fan Q, Li Q, Zhou S, Li L, Zhu Z and  
Lv X (2022) Source-Reservoir  
Characteristics and Accumulation of  
Gas Chimney-Type Gas Hydrates in  
Qiongdongnan Basin, Northern South  
China Sea.  
Front. Earth Sci. 10:880471.  
doi: 10.3389/feart.2022.880471

The Qiongdongnan Basin is an important gas hydrate exploration area in the South China Sea, but the gas hydrate accumulation process is poorly understood. By selecting an Lingshui (LS) target area and using first-hand geochemical data, three-dimensional seismic data, and an independent thermal insulation and pressure maintaining shipborne core analysis system, in this study, comprehensive geological evaluation was carefully conducted around the gas source and reservoir of the gas chimney hydrates, and the accumulation process was investigated. Geochemical data for a total of 47 sets of gas samples revealed that the gas source of the hydrates in the study area was mainly thermogenic gas supplemented by mixed gas. It was predicted that the contribution of the thermogenic gas to the hydrate accumulation was up to 70%. Using the independent shipborne core analysis system, the characteristics of the low-temperature combustible gas hydrates were determined, and the reservoir in the study area was characterized as non-diagenetic to weakly diagenetic, rich in clay and silt (D50 = 15.1–34.1 μm), weakly self-sustaining, and strongly heterogeneous. Based on the differentiated seismic response of the hydrate layer-gas bearing hydrate layer-shallow gas layer at the top of the gas chimney, the accumulation process in the target area was determined to be as follows: remote thermogenic gas transportation, local microbial genetic gas accumulation, episodic dynamic gas chimney reservoir formation, and source-reservoir control. In addition, the exploration ideas of an effective supply from a gas source and a shallow large-scale sand body are emphasized. The results of this study provide an important reference for the trial production of natural gas hydrates in the South China Sea.

**Keywords:** Qiongdongnan Basin, gas hydrates, gas chimney, gas source, reservoir, accumulation process

## 1 INTRODUCTION

Natural Gas Hydrates (NGHs) are a type of ice-like cage structure formed by water and natural gas molecules under low temperature and high pressure conditions. They mainly occur in dispersed, nucleated, vein-like, and massive forms in the seabed and at depths of >300 m in terrestrial permafrost regions in passive continental margins. Countries continue to pay attention to and invest in the research and development of natural gas hydrates, which are a strategic clean energy source. Gas hydrates have been found in 240 locations around the world. Hydrate pilot production has been

completed in Mackenzie in Canada, the north slope of Alaska, the Nankai trough in Japan, and the South China Sea (Paganoni et al., 2019; Wei et al., 2019; Deng et al., 2021; Lai et al., 2021).

Chinese gas hydrate surveying began in 1999. After long-term exploration and sea trials, NGHs have been identified as the 173rd new mineral. The Qiongdongnan Basin and the Pearl River Basin are delineated as two pilot test areas for natural gas hydrate exploration and production (Zhu et al., 2009; Zhang et al., 2019a). The research on exploration technology, reservoir formation mechanisms, and basic physical properties has reached or approaches the international advanced level, but the overall exploration degree is low. At present, the most important work is to establish reliable natural gas hydrate resource evaluation and exploration techniques. Since 2017, China has completed several rounds of offshore gas hydrate drilling, logging while drilling, and coring operations in the deep water area of the Qiongdongnan Sea area using the drilling and logging system on the independent offshore oil 708 deep water engineering survey ship and independently developed coring technology. Comprehensive domestic technologies and a complete operation process of the ship exploration drilling, logging, and coring evaluation sea test have been developed, making China the third country in the world to independently master this type of technology. After three rounds of voyage, Qiongdongnan Sea Area containing the hydrate formation of “strong BSR seismic reflection, high resistivity and low acoustic time” features, can be divided into “type gas chimney that are rich in thermogenic gas hydrate, polygons that are rich in thermogenic gas fracture—silt composite hydrate and the causes of thermogenic gas and mixed gas hydrate sliding body at the bottom of the” three kinds of hydrates. But the study on the geological process of accumulation is not enough.

The Qiongdongnan Basin is an important oil- and gas-producing area and hydrate-rich region in the South China Sea. The X17-2, X25-1, and X18-1 gas fields and the Haima active cold seep have been discovered successively along the channel of the central canyon of the basin, indicating that the deep gas source supply is sufficient and there are good transport channels and a favorable reservoir formation environment (Xu et al., 2016; Wang et al., 2018; Yang et al., 2018; Zhang et al., 2019b; Wan et al., 2020; Wei et al., 2020; Zhang et al., 2021; Chen et al., 2022). In particular, leaky gas hydrates, represented by gas chimney hydrates, have become one of the research objects in trial production projects (Zhang et al., 2016; Paganoni et al., 2019; Wei et al., 2019; Zhang et al., 2020a; Zhang et al., 2020b; Deng et al., 2021; Lai et al., 2021; Wan et al., 2021). However, gas chimney hydrates are characterized by multi-stage dynamic accumulation, multi-solution of logging seismic responses, strong reservoir heterogeneity, and low saturation of the ore body, which restrict our geological understanding and exploration techniques (Zhu et al., 2009; Wang et al., 2015; Wan et al., 2017; Wang et al., 2018; Wan et al., 2022).

In this study, the gas source, reservoir, and accumulation process of gas hydrates in the selected gas chimney hydrate enrichment area in the Lingshui(LS) sea area in the Qiongdongnan Basin were systematically and carefully investigated using first-hand geochemical and geophysical data. In terms of gas source, this is the first time that China's independent coring technology is used to collect and analyze

the gas data of hydrate formation in hydrate well and conventional gas layer in gas well, which is of practical significance to the co-production of hydrate and conventional gas and the correlation analysis of hydrate and conventional gas. In terms of reservoir, the infrared imaging characteristics, scanning electron microscopy and remolding characteristics of hydrate reservoir in previous studies are supplemented, and the fine grain characteristics and physical properties of hydrate reservoir are reported. A quantitative understanding of the gas source (70% thermogenic gas and 30% mixed gas) was obtained; two main reservoir types (rich silt shale (clay) reservoir and microfracture reservoir), were identified; and the “remote thermogenic gas filling gas chimney, local microbial origin supplementation, episodic dynamic accumulation, and source-reservoir control” accumulation mechanism was identified. The exploration idea of a gas source and sand body was determined to have a great potential. The results of this study provide an important scientific reference for the trial production of natural gas hydrates in the South China Sea.

## 2 GEOLOGIC BACKGROUND

The Qiongdongnan Basin is located at the west end of the continental shelf of the South China Sea, north of Hainan Island, south of the Yongle uplift of the Paracel Islands, west of the Yinggehai Basin, and adjacent to the Shenhu uplift and the Zhu III and Zhu II depressions. It is a NE-trending extensional rift sedimentary basin with a basin area of  $8.3 \times 10^4 \text{ km}^2$ . It consists of five secondary structural units: the Hainan uplift, northern depression, central uplift, central depression, and southern uplift. Because the Mesozoic, the Qiongdongnan Basin has experienced the Shenhu movement, the South China Sea movement, and the Dongsha movement successively, the sedimentary strata are characterized by three stages of differentiation: the Late Cretaceous-Late Oligocene multi-episode rifting period, the Early Miocene-Middle Miocene thermal subsidence period, and the Neotectonic period since the Late Miocene (Liang et al., 2019; Paganoni et al., 2019; Wei et al., 2019; Ye et al., 2019; Deng et al., 2021; Lai et al., 2021).

At present, the Qiongdongnan deep water area has become a key area for conventional oil and gas exploration and hydrate trial production, with a deep water area of about  $5.3 \times 10^4 \text{ km}^2$  and a maximum water depth of 3,000 m, including the central depression, the Songnan low uplift, and the Lingnan low uplift. The faults in the deep water area of the Qiongdongnan Basin are mainly developed in Paleogene strata, and the faults mainly trend NE-SW, E-W, and NW-SE. Among them, the large-scale NE-SW faults run through the central depression, with a length of about 300 km in the deep water area; and they divide the central Canyon waterway into the Ledong section, Lingshui section, Songnan section, and Baodao section. The deep water area of the basin exhibits a structural pattern characterized by north-south zoning and east-west partitioning (**Figure 1**) (Huang et al., 2016; Huang et al., 2017).

The study area is located in the Songnan low uplift area and is surrounded by the Lingshui Sag and the Beijiao Sag, with water

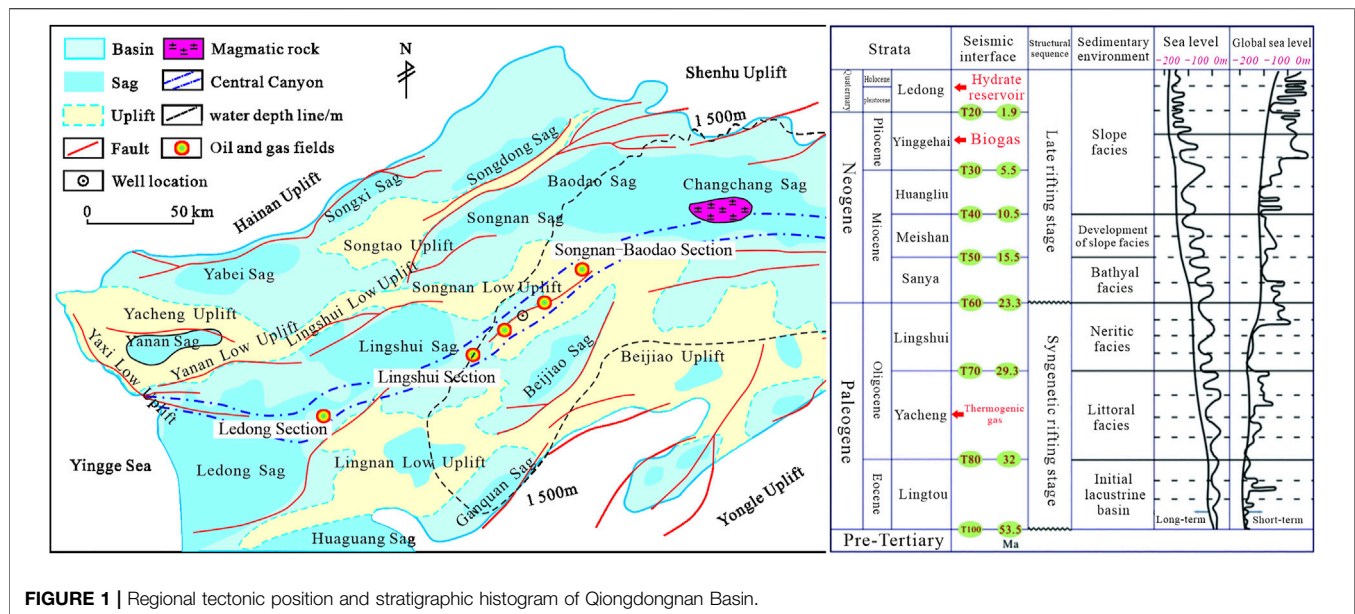


FIGURE 1 | Regional tectonic position and stratigraphic histogram of Qiongdongnan Basin.

depths of 1,650 m–1800 m. The focus of the exploration is the gas chimney group in the Songnan low uplift. The 3D seismic data and general survey reveal that this area has geological characteristics indicative of gas hydrate accumulation. 1) High production gas flow has been obtained from an exploration well adjacent to the X17-2 gas field in the submarine fan sandstone reservoir of the Neogene Yinggehai Formation, with a daily gas output of  $110 \times 10^4 \text{ m}^3$ , which is the first large deep water gas field covering over 100 billion cubic meters discovered by CNOOC. 2) Multiple gas chimneys are distributed in the Ne-trending belt; a typical blank zone reflection and BSR distribution can be seen in the structure. The geothermal gradient of the gas chimneys is high ( $113^\circ\text{C}/\text{km}$ ), the transport system is well developed, and the fluid circulation is active. 3) The hydrates are mainly developed in the submarine fan silt-sand reservoir in the Quaternary Ledong Formation, the provenance of which includes the Kunsong Block, Red River in India, and Hainan Island. 4) Remotely Operated Vehicle (ROV) observations revealed that the terrain of the seafloor is flat, with a small number of pock marks and deep-sea organisms. Crustacean fragments were observed around the pocks.

### 3 METHODS

In this study, 47 representative samples were systematically collected from hydrate wells and conventional exploration wells in the study area, and they were subjected to gas source analysis, including data on the gas components and carbon isotope compositions of the methane in the deep, medium, and shallow strata in the gas chimney development areas, such as areas X18-H5 and X17-2. The gas composition was analyzed by gas chromatography mass spectrometer. The carbon isotope was analyzed by stable isotope mass

spectrometer. The water depth of the sampling well is 1720 m, and the hydrate occurrence depth is 24–172 mbsf. The well is located above the core of the gas chimney. Based on the identification chart for hydrocarbon gas genetic types in marine sediments, the genetic discrimination was conducted using the samples' gas humidity values,  $k = C1/(C2+C3)$ , the carbon isotope compositions of the methane and ethane in the gas samples.

The reservoir in the Qiongdongnan Sea Area has been carefully analyzed using an independent ship-borne thermal insulation and pressure preserving core analysis and testing system developed in China. To confirm the low temperature and flammability of the methane hydrates, a portable infrared thermal imager was used to core the hydrate enrichment intervals from 127 to 153 mbsf. The sediment particle sizes of 15 samples from different depths (0–173 mbsf) were analyzed using a shipboard laser particle size analyzer (BT-9300ST, Dandong Bettersize Instruments Co., Ltd., Dandong, China). According to the national standard (GB/T19077.1-2008), sediment samples weighing 0.5 g were added to 1,000 ml of deionized water, and then 0.5 M sodium hexametaphosphate was added as the dispersant. After that, the samples were stirred for at least 1 min to evenly disperse the particles. Finally, the samples were dried and tested. The rock and mineral analysis of the sediment samples from 151.7 mbsf was conducted using a shipboard X-ray diffractometer. In addition, the samples were observed using a scanning electron microscope (SEM) (Nova NanoSEM 450, FEI Co., United States of America). Ten grams of the sample was weighed and dried, and then, a small spoonful of dry sample was smeared on tape for field emission SEM measurements. *In situ* X-ray Computed Tomography (CT) scans (SMX-225CTX-SV, Shimadzu Co., Japan) were performed on samples from depths of 120 and 123.5 mbsf under pressure with a resolution of 40  $\mu\text{m}$ .

## 4 RESULTS

### 4.1 Characteristics of the Gas Source of the Natural Gas Hydrates

#### 4.1.1 Gas Composition and Isotope Characteristics

It can be seen from the test results of the samples from the deep, medium, and shallow strata that the main components of the gas include hydrocarbon gases, such as methane, ethane, and propane, and non-hydrocarbon gases, such as carbon dioxide, sulfur dioxide, and nitrogen. The methane content is the highest (97.7%, average of 89.21%, excluding four shallow samples from

area X25-1), and the ethane content is also high(17.01%, average of 7.88%, excluding four shallow samples from area X25-1). The average carbon dioxide content was 1% (Table 1) (Huang et al., 2016; Huang et al., 2017; Cong et al., 2018; Liang et al., 2019; Paganoni et al., 2019; Wei et al., 2019; Ye et al., 2019; Deng et al., 2021; Lai et al., 2021). Therefore, the gas composition shows that Type I and II methane hydrates are developed and occur in the study area (Figure 2). The carbon isotope values of the methane are  $-59.5\text{‰}$  to  $-35.4\text{‰}$ , with an average of  $-46.26\text{‰}$ . The carbon isotope values of the ethane are  $-20.67\text{‰}$  to  $-27.6\text{‰}$ , with an average of  $-25.22\text{‰}$ . The humidity values of the samples are

**TABLE 1 |** Gas composition and isotope data of gas chimney type hydrate in Qiongdongnan Basin (Huang et al., 2016; Huang et al., 2017; Cong et al., 2018; Liang et al., 2019; Paganoni et al., 2019; Wei et al., 2019; Ye et al., 2019; Deng et al., 2021; Lai et al., 2021)

No.	Sample	Sample type	Depth/mbsf	C <sub>1</sub> /%	C <sub>2</sub> /%	CO <sub>2</sub> /%	δC <sub>1</sub> /‰	δC <sub>2</sub> /‰	C <sub>1</sub> /(C <sub>2</sub> +C <sub>3</sub> )	Maker	Source
1	X18-H5-1	Hydrate gas	27.2	83.08	13.54	3.38	-58.7	-23.07	6	CNOOC	This study
2	X18-H5-2	Hydrate gas	67.2	95.83	4.17	0	-58.47	-22.95	23	CNOOC	This study
3	X18-H5-3	Hydrate gas	129.7	86.64	11.5	1.86	/	/	8	CNOOC	This study
4	X18-H5-4	Hydrate gas	147.2	92.93	6.3	0.77	/	/	15	CNOOC	This study
5	X18-H5-5	Hydrate gas	151.7	81.85	15.8	2.35	/	/	5	CNOOC	This study
6	X18-H5-6	Hydrate gas	172	86.17	13.51	0.32	-48.08	-20.67	6	CNOOC	This study
7	X25-1-1	Deposits	37	10.22	0.46	0.02	-46.2	-27.6	22	CNOOC	This study
8	X25-1-2	Deposits	37.2	3.55	0.18	0.04	-45.9	-24.3	20	CNOOC	This study
9	X25-1-3	Deposits	37.4	8.12	0.16	0.05	-46.5	-25.5	51	CNOOC	This study
10	X25-1-4	Deposits	37.6	2.64	0.12	0.06	-46.7	-26.9	22	CNOOC	This study
11	X25-1	Natural gas	Huangliu	83.66	7.2	5.98	-38.3	-24.8	13	CNOOC	Gan et al., 2018
12	X25-2	Natural gas	Huangliu	77.81	6.84	4.29	-35.4	-25.2	14	CNOOC	Gan et al., 2018
13	X25-5	Natural gas	Huangliu	79.93	8.23	2.6	-41.6	-26.1	15	CNOOC	Gan et al., 2018
14	X17-2-1	Natural gas	3,306	92.51	6.14	0.45	-36.8	-23.5	15	CNOOC	Huang et al. (2016)
15	X17-2-2	Natural gas	3,329	91.68	5.9	0.7	-38.2	-23.7	16	CNOOC	Huang et al. (2016)
16	X17-2-3	Natural gas	3,407	89.45	7.21	0.53	-38.0	-25.3	12	CNOOC	Huang et al. (2016)
17	X17-2-4	Natural gas	3,251	90.97	7.68	0.2	-39	-25.4	12	CNOOC	Huang et al. (2016)
18	X18A-1	Natural gas	Huangliu	88.01	6.89	0.06	-40.1	-26.4	16	CNOOC	Gan et al., 2018
19	X18A-2	Natural gas	Huangliu	89.30	5.95	0.05	-40.4	-25.2	17	CNOOC	Gan et al., 2018
20	X18B-1	Natural gas	Huangliu	94.15	3.67	0.05	-40.4	-25.2	18	CNOOC	Gan et al., 2018
21	X22-1-1	Natural gas	3,339	91.16	7.48	0.31	-39.2	-26.2	19	CNOOC	Liang et al., 2016
22	X22-1-2	Natural gas	3,352	91.37	7.28	0.32	-38.8	-26	20	CNOOC	Liang et al., 2016
23	X22-1-3	Natural gas	3,391	91.53	7.20	0.32	-39.2	-26	21	CNOOC	Liang et al., 2015
24	W08-2018-1	Hydrate gas	8	97.69	2.05	/	-59.5	-26.0	46	CGS	Lai et al. (2021)
25	W08-2018-2	Hydrate gas	62.93	81.21	12.88	/	-56.3	-26.9	5	CGS	Lai et al. (2021)
26	W08-2018-3	Hydrate gas	148.4	79.16	14.4	/	-50.4	-26.5	4	CGS	Lai et al. (2021)
27	W08-2018-4	PCS	32.88	94.94	4.23	/	-54.4	-25.5	19.7	CGS	Lai et al. (2021)
28	W08-2018-5	PCS	79	95.75	3.69	/	-58.6	-25.1	23.5	CGS	Lai et al. (2021)
29	W08-2018-6	PCS	80.9	95.73	3.68	/	-48.8	-22.4	23.7	CGS	Lai et al. (2021)
30	W08-2018-7	PCS	112.3	96.46	2.99	/	-53.8	-23.3	29.1	CGS	Lai et al. (2021)
31	W08-2018-8	PCS	145.65	83.49	11.61	/	-49.3	-27.5	5.4	CGS	Lai et al. (2021)
32	W08-2018-9	PCS	158	84.17	10.99	/	-50.4	-26.9	5.7	CGS	Lai et al. (2021)
33	W08-2018-10	PCS	187.1	92.82	4.56	/	-50.4	-26.7	14	CGS	Lai et al. (2021)
34	W9B-2018-1	Void gas	18.55	95.2	4.22	/	/	/	22	CGS	Liang et al. (2019)
35	W9B-2018-2	Void gas	42	88.3	9.71	/	/	/	8	CGS	Liang et al. (2019)
36	W9B-2018-3	Void gas	43.98	90.4	7.98	2978 ppm	/	/	10	CGS	Liang et al. (2019)
37	W9B-2018-4	Void gas	59.12	98.3	1.33	1687 ppm	/	/	68	CGS	Liang et al. (2019)
38	W9B-2018-5	Void gas	59.9	98.3	1.31	1776 ppm	/	/	70	CGS	Liang et al. (2019)
39	W9B-2018-6	Void gas	73.18	95.1	4.50	/	/	/	20	CGS	Liang et al. (2019)
40	W9C-2018-1	Void gas	106	97.3	2.40	/	/	/	40	CGS	Liang et al. (2019)
41	W9C-2018-2	Void gas	107	97.7	2.07	1088 ppm	/	/	46	CGS	Liang et al. (2019)
42	W9C-2018-3	Void gas	131.81	81.6	15.04	700 ppm	/	/	5	CGS	Liang et al. (2019)
43	W9C-2018-4	Void gas	133.61	86.9	11.31	/	/	/	7	CGS	Liang et al. (2019)
44	W9C-2018-5	Void gas	152.29	79.1	16.56	2339 ppm	/	/	4	CGS	Liang et al. (2019)
45	W9C-2018-6	Void gas	152.69	78.5	17.01	2216 ppm	/	/	4	CGS	Liang et al. (2019)
46	W9C-2018-7	Void gas	155.14	84.5	11.38	2142 ppm	/	/	6	CGS	Liang et al. (2019)
47	W9C-2018-8	Void gas	156.21	85.6	10.51	1880 ppm	/	/	6	CGS	Liang et al. (2019)

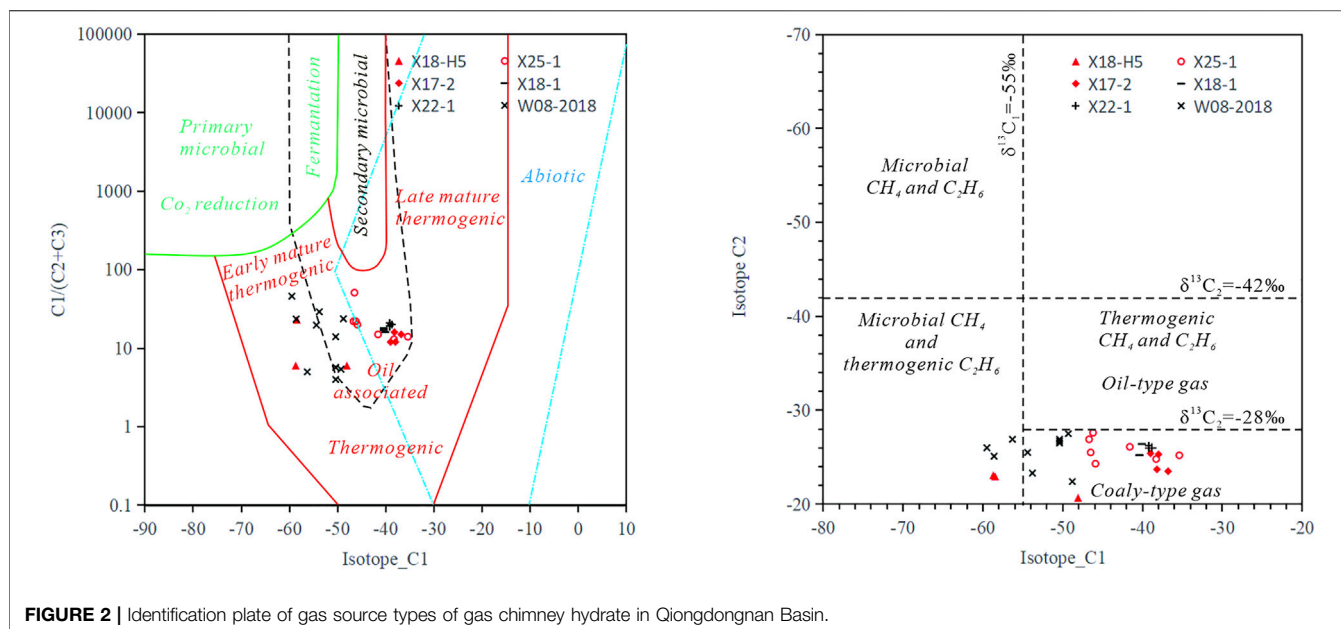


**FIGURE 2** | Identification plate of gas source types of gas chimney hydrate in Qiongdongnan Basin.

4–51, with an average of 17.8. From the relationship between the gas composition and depth, it can be seen that the methane contents of the shallow samples are higher than those of the deep samples, and the ethane contents of the deep samples are higher than those of the shallow samples. The contributions of the deep thermogenic gas and shallow microbial gas to the gas components are shown in **Figure 3**.

#### 4.1.2 Gas Source Types and Contributions

The isotopic error analysis revealed that the original signal is clearly retained in the isotopic data for the collected samples. The first gas origin chart (Milkov and Etiop, 2018) divides the gas into primary microbial origin, low microbial origin, thermal origin, and abiogenic origin. The majority of the gas samples plot in the oil-type thermal origin gas and early maturation thermal origin gas fields (**Figure 2**). On the second gas origin chart (Huang et al., 2016; Huang et al., 2017; Cong et al., 2018; Liang et al., 2019; Paganoni et al., 2019; Wei et al., 2019; Ye et al., 2019; Deng et al., 2021; Lai et al., 2021; Zhang et al., 2020), the majority of the gas samples plot in the coal-derived thermogenic methane and ethane fields, and only four samples plot in the microbiological methane and thermogenic ethane fields (mixed gas) (**Figure 2**). Both of these results confirm a thermogenic gas origin, but there are limitations to the coal type pyrolysis gas and oil type pyrolysis gas (i.e., they are significantly different in terms of the chemical composition and structure of the gas forming parent material). Combined with the sample properties and identification results, it is concluded that the hydrate gas in the study area is mainly thermogenic gas, supplemented by mixed genetic gas, and the contribution of the thermogenic gas is 70%.

#### 4.1.3 Gas Resource Potential

The comparison of the gas source revealed that the source rocks of the biogenic gas in the study area are the marine siltstone and

argillaceous siltstone of the local Yinggehai Formation-Quaternary system. The carbon isotope compositions of the methane range from  $-87\text{‰}$  to  $-62\text{‰}$ , and the organic carbon contents of the source rocks of the gas range from 0.28 to 0.49%. The thermogenic gas in the study area is derived from the source rocks of the Yacheng Formation to Sanya Formation in the Lingshui Sag and Beijiao Sag. The organic matter is Type II and III kerogen and is in the mature to highly mature ( $R_o = 1.6\text{--}3.5\%$ ) gas-generation stage. It is concluded that the gas source in this area is sufficient and can serve as the basis for mineralization.

## 4.2 Characteristics of Gas Hydrate Reservoir

The reservoir in the study area is composed of the clayey silty and silty clay deposits of the Quaternary Ledong Formation ( $\sim 1.9$  Ma), which is a non-diagenetic fine-grained reservoir in the abyssal plain facies. The natural gamma ray values of the hydrate formation are 30–50 API higher than those of the adjacent formation. The content of silty sand is high, but it is still in the clay-silty sand grade for weak diagenetic-non-diagenetic and quartz-rich feldspar. It was found that the hydrate reservoir is weakly diagenetic to non-diagenetic, is rich in clay and silt, is weakly self-sustaining, and is strongly heterogeneous.

### 4.2.1 Thermal Imaging Characteristics of Hydrate Cores

At room temperature (about  $27^\circ\text{C}$ ), the temperature range of the core samples is  $-3.1$  to  $30^\circ\text{C}$ , and the temperatures of the columnar thermal insulation and pressure retaining reservoir samples are  $23\text{--}25^\circ\text{C}$ . The block hydrate samples have

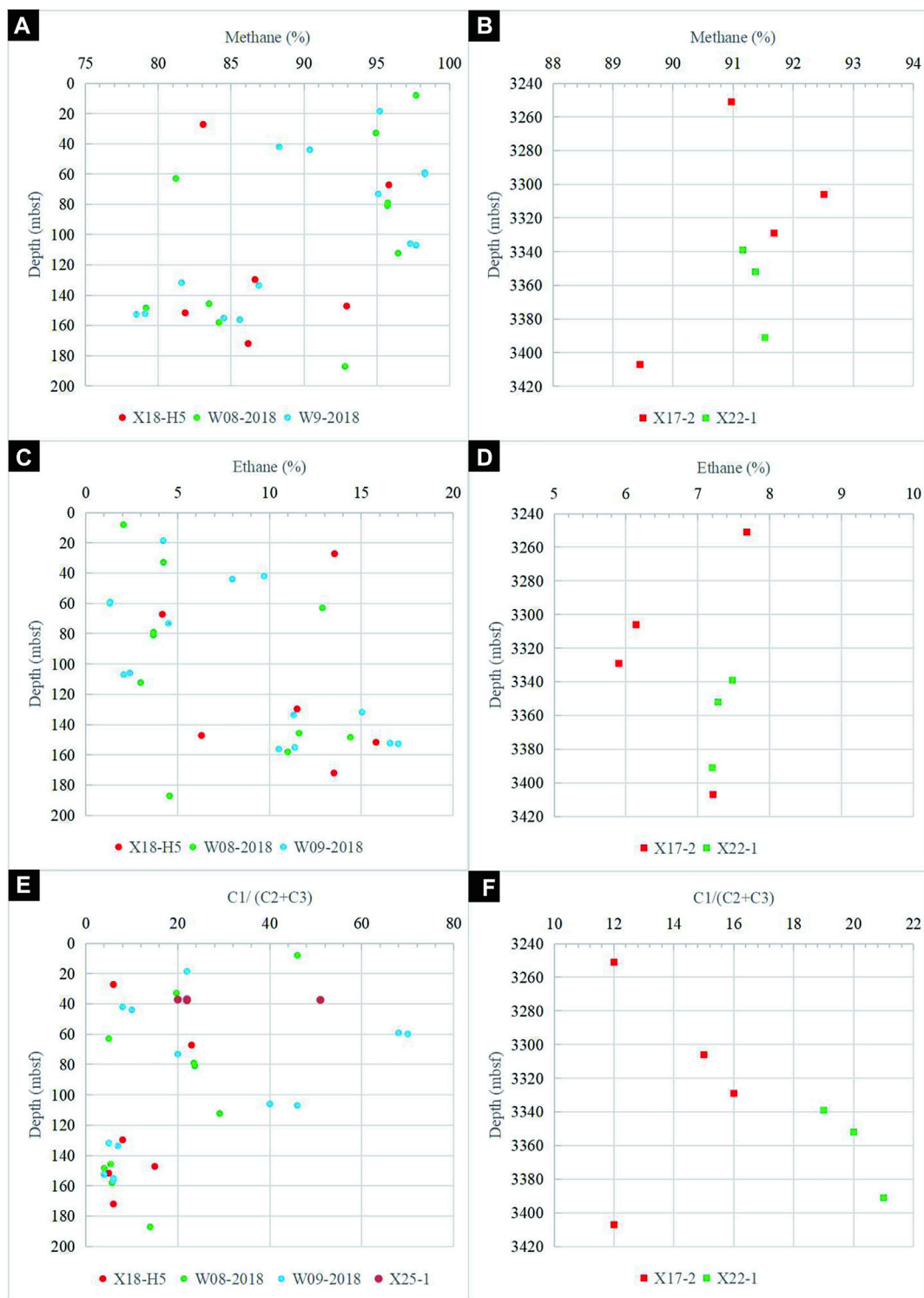


**FIGURE 3 |** Gas content at different depths at different sites (A,B) Methane; (C,D) Ethane; (E,F) C1/(C2+C3)

significant low temperature characteristics ( $-3.1-0^{\circ}\text{C}$ ), and they were compared with the flame temperature of the hydrate after ignition ( $89^{\circ}\text{C}$ ), which proves that the hydrates are characterized by low-temperature flammability. The overall shape of the

reservoir is cylindrical (purple, about  $25-26^{\circ}\text{C}$ ), and the hydrate ore body has a low temperature (black, about  $1.6^{\circ}\text{C}$ ) and is distributed in patches and masses, indicating that the coring harvest was basically complete (Figure 4).

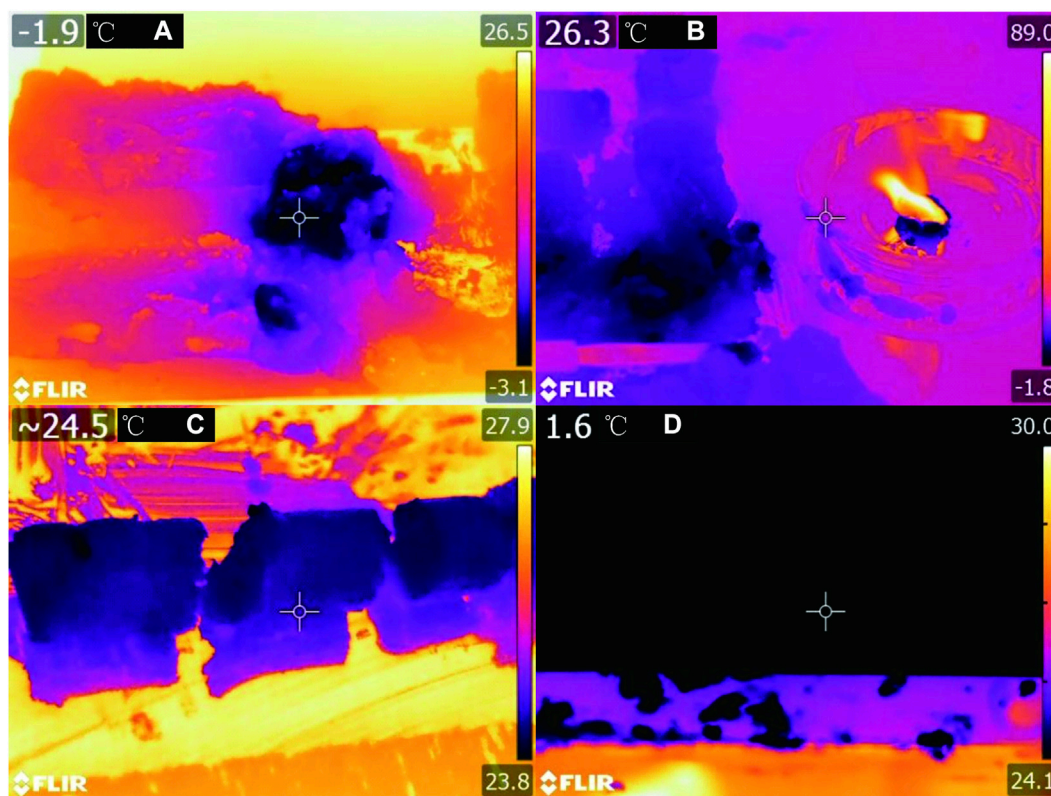


**FIGURE 4** | Core thermal imaging characteristics (A) hydrate measurement; (B) flame measurement; (C) Columnar core measurement; (D) ore body measurement).

During the process of transferring the sample from the temperature and pressure environment, 1) in the initial stage of core removal, the reservoir exhibited a good cylindrical shape, but the cylindrical samples gradually collapsed during the subsequent testing process, with scattered and porridge-like characteristics. This indicates that the reservoir is non-diagenetic to weakly diagenetic and is poorly self-sustaining. The hydrates play an important role in supporting the stable consolidation of the reservoir's framework. 2) Several independent and dispersed hydrate ore bodies were observed in the obtained multi-section rock core, indicating the poor connectivity and strong heterogeneity of the hydrate reservoir. 3) During the core placement, the temperature of the reservoir continued to increase, which is speculated to have been caused by the decomposition and heat absorption of the dispersed hydrates in the reservoir's pores.

#### 4.2.2 Particle Size Analysis

The particle size analysis results are presented in **Table 2**. The results show that 1) the median grain size of the sediments ranges from 15.1 to 34.1  $\mu\text{m}$ , and the median grain size is concentrated in the range of 21.3–28.9  $\mu\text{m}$  (9/15), indicating that the reservoirs are composed of silty sediments. 2) At sampling depths of 0.8 mbsf and 123 mbsf, the median grain size of the reservoir is 30–34  $\mu\text{m}$ .

Combined with the Cone Penetration Test (CPT) stress characteristics at the corresponding depth, the analysis results indicate that the reservoir is composed of carbonate crust or a small amount of silty deposits, reflecting ancient cold seep activity. 3) The grain size of the sediments varies little with depth, indicating that the sedimentary environment is Quaternary deep-sea suspended sediments, and large-scale silty and sandy deposits are not present.

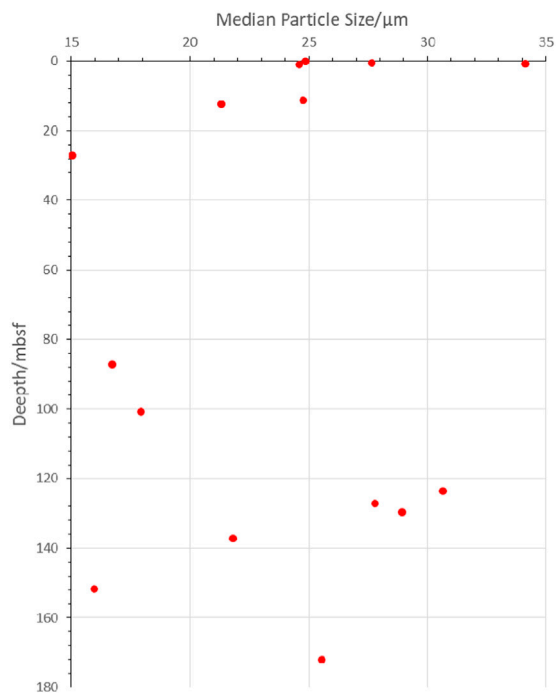
#### 4.2.3 Mineral Composition and Electron Microscopic Characteristics

The main mineral composition of the samples included quartz (23%), plagioclase (17%), sericite (15%), albite (14%), calcium carbonate (10%), illite (10%), potassium microcline (3%), pyrite (1%), and amphibole (1%). The corresponding major element compositions of the samples included silicon dioxide (54%), aluminum oxide (15%), calcium oxide (5%), ferric oxide (5%), potassium oxide (4%), magnesium oxide (3%), sodium oxide (2%), sulfur oxide (2%), and titanium dioxide (1%). The above results show that the main minerals in the samples were quartz, chlorite, mica, and feldspar, indicating that the reservoir is a clay-rich silty deposit.

A large number of lamellar clay minerals were observed under the electron microscope, but the mineralization and

**TABLE 2** | Sample depth and median grain size of gas chimney type gas hydrate reservoir in Qiongdongnan Sea Area.

Depth(m)	median grain size( $\mu\text{m}$ )
0.1	24.856
0.5	27.641
0.8	34.112
0.95	24.600
11.2	24.760
12.3	21.312
27.2	15.055
87.2	16.710
100.7	17.946
123.7	30.642
127.2	27.784
129.7	28.944
137.2	21.804
151.7	15.962
172	25.555



diagenetic characteristics of the minerals were weak, indicating that the reservoir is weakly diagenetic to non-diagenetic (Figure 5).

**4.2.4 Pore Structure and CT Scans**

*In situ* X-ray CT analysis yielded two typical reservoir structural features that were consistent with the predicted major reservoir types (Figure 6). Figure 6A shows the clay-

rich silty reservoir lacking fractures, and it is fine grained and homogeneous overall (gray). The inferred hydrate ore body (black) is massive and porphyritic and is independently dispersed within the core, lacking a continuous veined core. Figure 6B shows the clay-rich silty reservoir with well-developed fractures. Overall, the fractures (dark brown) are well developed and have inconsistent strikes. A small amount of granular hydrate (black) can be seen in the core fractures, but

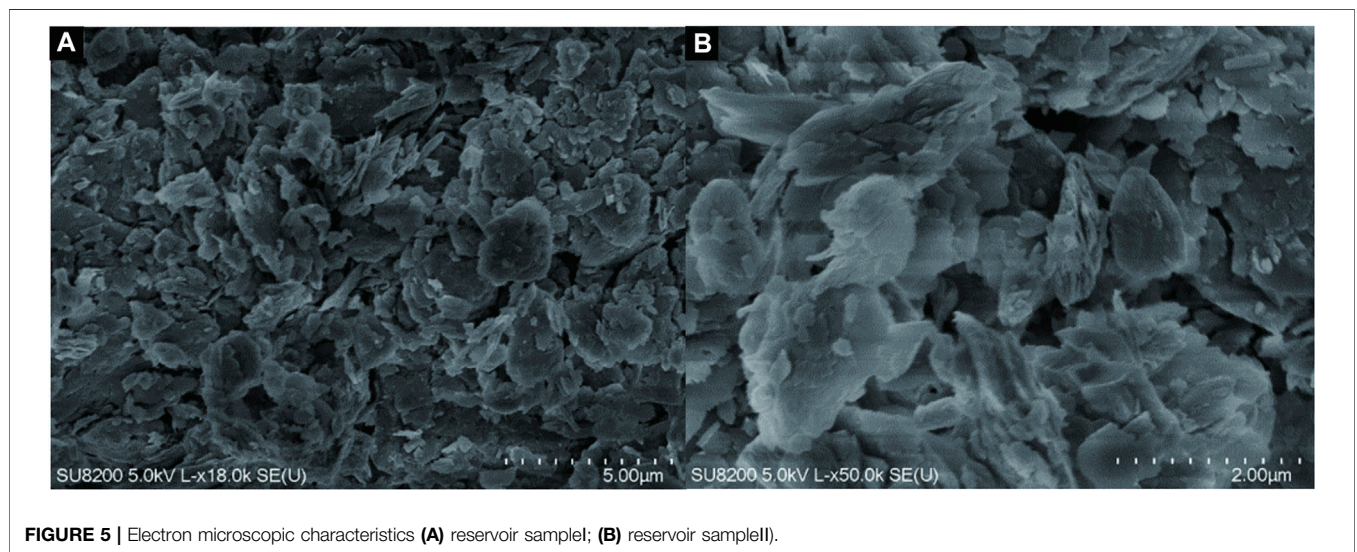


**FIGURE 5** | Electron microscopic characteristics (A) reservoir sampleI; (B) reservoir sampleII).



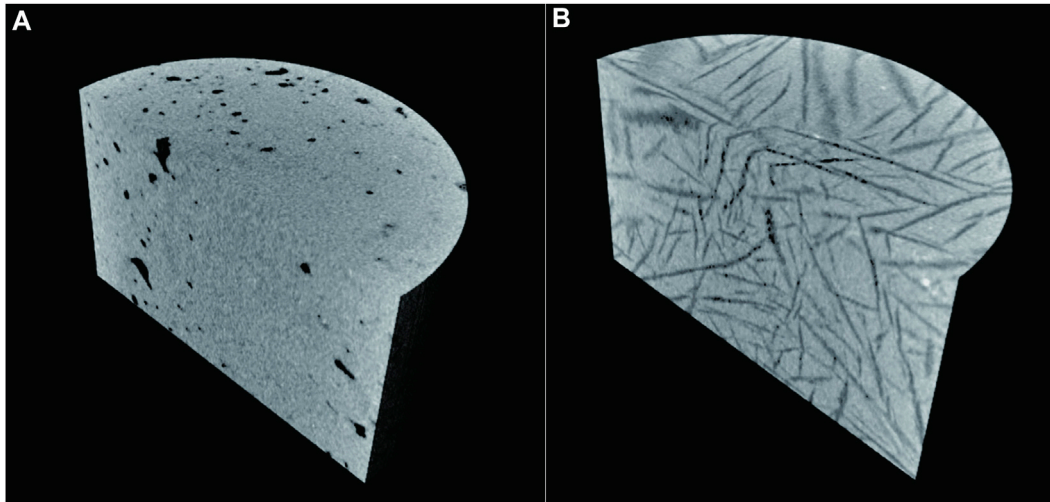


**FIGURE 6** | 3D simulated images of two types of reservoirs by X-ray CT scanning (A) reservoir sample; (B) reservoir sample II).

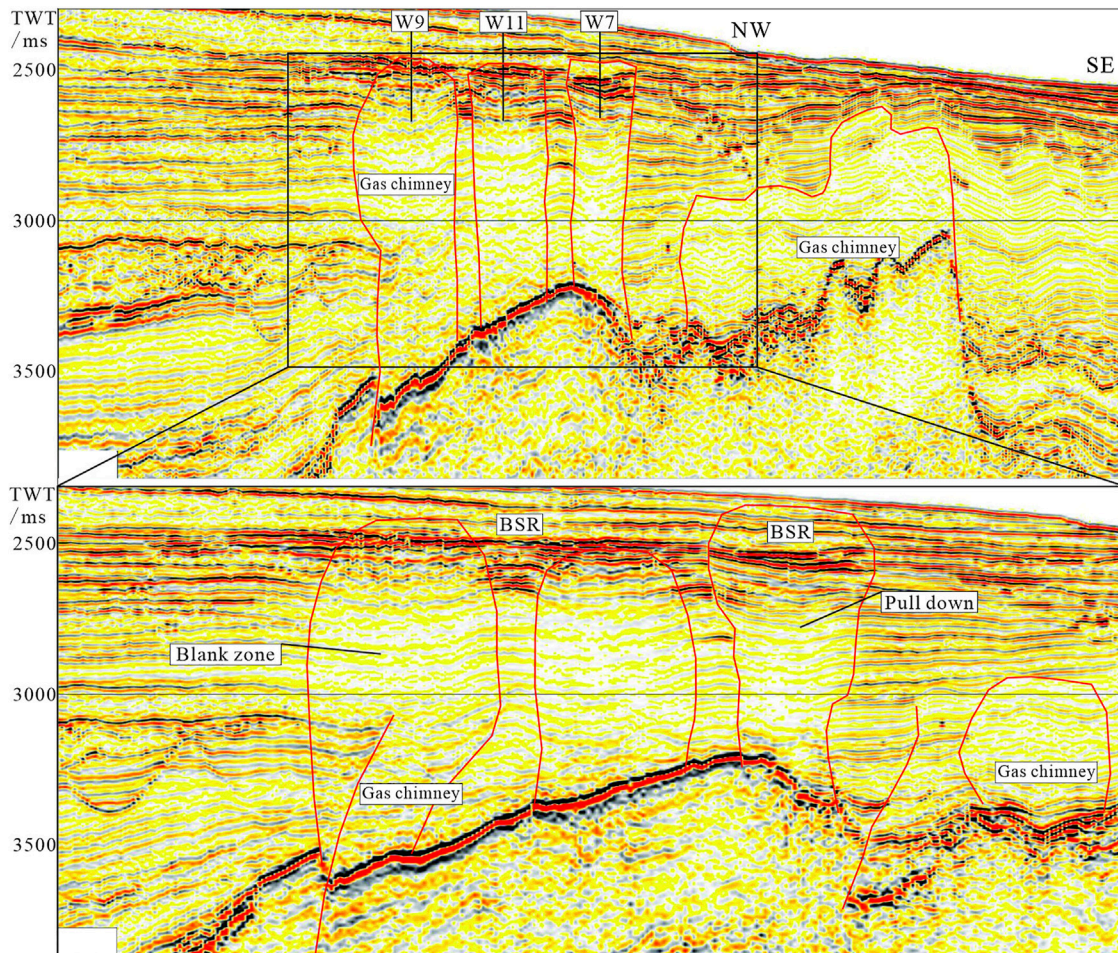


**FIGURE 7** | Seismic reflection of gas chimney structure in H area of Qiongdongnan Basin.

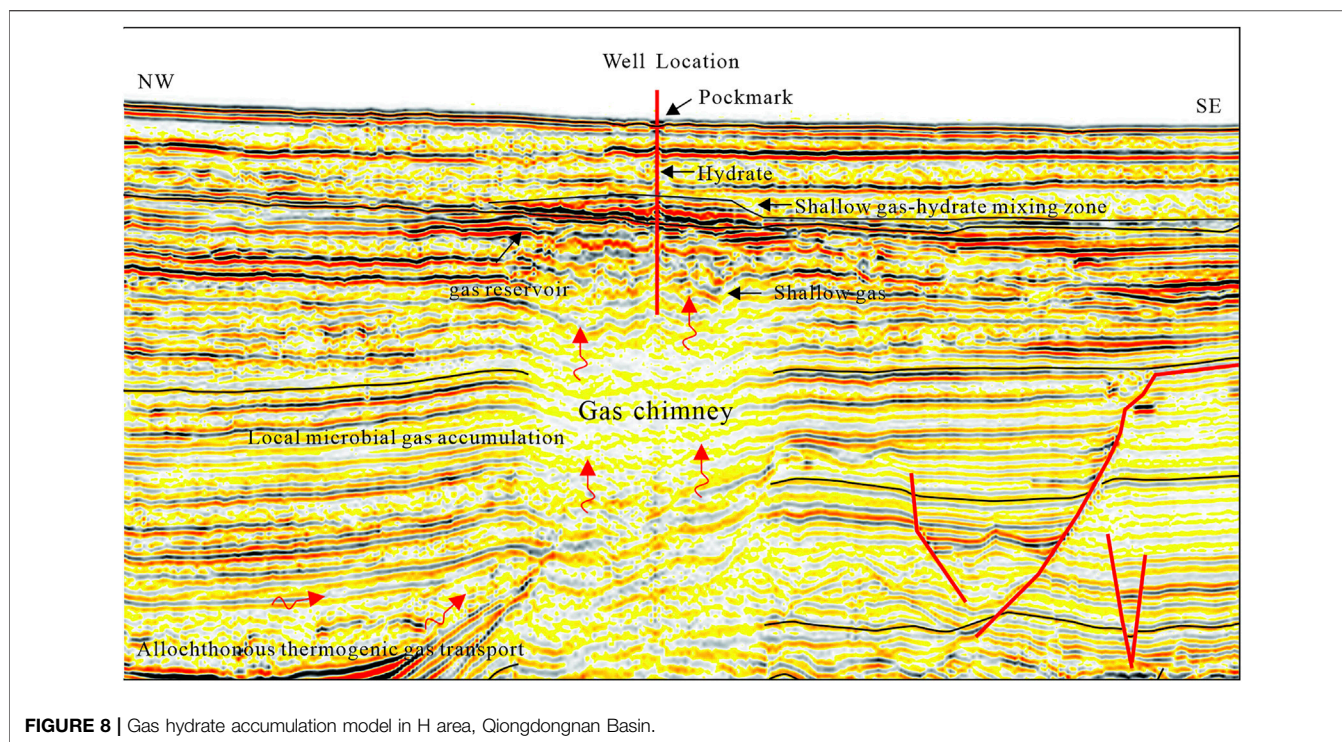


**FIGURE 8** | Gas hydrate accumulation model in H area, Qiongdongnan Basin.

the amount of nucleation is limited. It was found that the microfracture reservoir is the main reservoir type in the gas chimney, and the fractures improve the hydrate storage space, which suggests that research on fractured reservoirs in fine-grained sediments should be strengthened.

## 5 DISCUSSION

### 5.1 Gas Chimney Conductor

Gas chimney-type hydrates are the main occurrence structure of the gas hydrates in the Qiongdongnan Sea Area. Gas chimneys are often formed by overpressure of the gas reservoir, low structural stress, and mud shale isolation. In fact, they are microfracture groups formed by abnormal formation pressure that appear as oval or upright chimneys on the seismic profile. They are characterized by abnormal velocities, in-phase axis pull down, and chaotic blank reflections due to the gas they contain (Figure 7) (He et al., 2015; Zhang et al., 2019). Theory and exploration have revealed that the evolution of mud diapirs, gas chimneys, and pocks is continuous, and these structural groups have a high fluid transport efficiency. The characteristics of gas chimneys can reflect the tectonic evolution stage of the gas chimneys, the fluid flux, and the migration path.

The gas chimneys in the LS region are concentrated in the ridges of the Songnan low uplift. The diameters of the individual gas chimneys are 3–7 km, and four consecutive gas chimneys form a group along the NEE direction. The tops of the gas chimneys are wide and low and are covered by Quaternary argillaceous deposits and silt-rich slump bodies. The bottom simulating reflector (BSR) phenomenon is obvious in the

submarine fan of 3rd Ledong Formation and the 4th Ledong Formation. The acoustic Blank Zone (BZ) in the core of the gas chimney is long and elliptic and exhibits a wave impedance difference with the surrounding rock. The core is often connected with the sand body, and the root narrows, and it is in unconformable contact with the underlying strata (Figure 8).

Based on the geological and geophysical analysis, the gas chimneys are considered to be the most efficient known transport channels in this area. The study area has a high geothermal gradient (65°C/km in the wing and 113°C/km in the core). A large number of craters and biological remains of shellfish were observed on the seafloor, and carbonate crusts and bioclasts were repeatedly returned with the rock debris, indicating that fluid channels developed in the tops of the gas chimneys and there is upwelling and paleo-cold seep activity. In addition, a large number of fractures were observed in the remolded cores, indicating that abnormal fluid pressure played an important role in the formation of the large-scale fractured reservoirs.

In particular, combined with the logging data, the seismic profile can be divided into a hydrate layer (top), a hydrate and shallow gas mixed layer (middle), and a shallow gas layer (bottom). The gas hydrates in the upper member of the Ledong Formation at the top of the gas chimneys exhibit a scattered, patchy, strong amplitude and in-phase axial thickening, and the BSR is more obvious. The gas-water transition zone in the middle part of the Ledong Formation is characterized by multiple sets of external wedge-shaped filling deposits and a strong internal amplitude. Based on the core of the lower member of the Ledong Formation, the larger the free gas content is, the more obvious the pull-down amplitude of the isophase axis is. This three-section characteristic and the logging

interpretation indicate that deep and local gas accumulated at the top after convergence and spilled down after saturation. The gas boundary is controlled by the temperature and pressure conditions, indicating that the scope of the gas charging and the reservoir configuration affect the scale of the hydrate occurrence.

## 5.2 Accumulation and Main Controlling Factors

Based on the above understanding, the geological process and a model of the gas hydrate accumulation in the study area were determined: remote thermogenic gas transportation, local microbial genetic gas accumulation, episodic dynamic gas chimney reservoir formation, and source-reservoir control. The analysis of the source of the gas revealed that multiple gas sources are the material basis of the gas chimneys. The gas source of the NGHs in the Songnan low uplift is mainly thermogenic gas from the remote Lingshui Sag, Lingshui Subsag, and Beijiao Sag. Based on the geothermal gradient and basin model, the Yacheng, Lingshui, and Sanya formations are in the oil-generation window (3,150–5,000 m, RO = 0.5–1.3%), and they have a thermogenic gas generation and hydrocarbon expulsion capacity (Zhang et al., 2019). Allochthonous thermogenic gas can be transported into the mud diapir through the sand channels, sheet sands, unconformity interface, and faults around the gas chimney, and the gas continuously accumulates in the weak zone of the mud diapir. The deep-sea argillaceous gas source rocks of the Meishan Formation, Huangliu Formation, Yinggehai Formation, and Quaternary Formation have entered the stage of microbial gas generation and also have hydrocarbon generation and expulsion capabilities.

Because the hydrocarbon expulsion time of the deep geothermal gas is much earlier than that of the shallow microbial gas (Zuo et al., 2016; Li et al., 2017; Song et al., 2021), the two types of gas and their mixture migrate, charge, and converge in stages. First, the thermogenic gas in the remote Yacheng Formation migrated over a long distance into the mud diapirs-gas chimneys along the sand body, unconformity interface, and faults under the action of overpressure, and the continuous charging of a large amount of thermogenic gas led to the development of microcracks in the mud diapirs-gas chimneys. Then, the local microbial gas preferentially migrated from the high fluid potential area to the low fluid potential area along the existing fracture groups and sand bodies in the hydrocarbon expulsion stage, and the gas chimneys continued to evolve under the sufficient gas supply conditions. Finally, the gas accumulated at the top of the gas chimney and was charged down and on the weak side, forming different types of hydrates under the favorable temperature and pressure conditions in the trap.

Episodic and dynamic reservoir formation is a new understanding of gas chimney gas hydrate exploration, which is mainly manifested as dynamic reservoir formation and the strong heterogeneity of the hydrates. In the longitudinal direction, the thermogenic gas and microbial gas experience episodic hydrocarbon expulsion migration and accumulation

processes. The gas can break through the surface and form an active cold seep (such as the Haima Cold Seep) during the peak of the hydrocarbon expulsion stage, and a migration channel is opened, which is conducive to the continuous development and enrichment of gas hydrates. In the low valley of the hydrocarbon expulsion stage, the migration channel is closed, and the cold seep can evolve into an ancient cold seep (a pock relic), resulting in the continuous decomposition and local diffusion of the hydrates. Such episodic reservoir formation is always in dynamic evolution and has been verified by multiple types of well data. The episodic and dynamic accumulation characteristics strengthen the contribution to the reservoir heterogeneity, which is beneficial to understanding the accumulation process.

In summary, the geological process of hydrate accumulation in the study area involves remote thermogenic gas transportation, local microbial genetic gas accumulation, gas chimney episodic dynamic reservoir formation, and source-reservoir control. Among them, the gas source determines the material basis of the hydrate accumulation, and the continuous charging and effective supply range of the gas are conducive to the stable development and accumulation of hydrates. The favorable reservoir determines the filling effect of the hydrate accumulation and the size and state of the ore body. Sand-rich reservoirs and fracture-rich reservoirs are favorable to the formation of a concentrated, high saturation ore body. The influences of the cap layer, conduction system, and temperature and pressure conditions are limited. Based on the above research results, we believe that the next step should be to strengthen research on the multi-source effective gas supply and deep-sea shallow sand body distribution to improve our geological understanding and exploration ideas.

## 6 CONCLUSION

- 1) Based on newly obtained geochemical data for 47 oil and gas wells and hydrate wells, it was found that the gas source of the gas chimney-type natural gas hydrates in the Qiongdongnan Basin is mainly thermogenic gas supplemented by mixed gas. Based on the samples, it was estimated that the contribution of the thermogenic gas to the hydrate accumulation was 70%.
- 2) The reservoirs in Qiongdongnan Basin were determined to be non-diagenetic to weakly diagenetic, rich in clay and silt (median grain size of 15.1–34.1  $\mu\text{m}$ ), weakly self-sustaining, and strongly heterogeneous. There are two main types of reservoirs: silty and argillaceous (clay) reservoirs and microfracture reservoirs.
- 3) Based on the seismic characteristics of the top of the gas chimney, i.e., a hydrate layer, gas hydrate-containing layer, and shallow gas layer, it was determined that the geological processes were as follows: remote thermogenic gas transportation, local microbial genetic gas accumulation, episodic dynamic gas chimney reservoir formation, and source-reservoir control. This suggests that the geological understanding and exploration ideas of an effective supply from a gas source and the distribution of deep-sea shallow sand bodies should be strengthened.

## DATA AVAILABILITY STATEMENT

The original contributions presented in the study are included in the article/Supplementary Material, further inquiries can be directed to the corresponding author.

## AUTHOR CONTRIBUTIONS

QF: main idea, writing-original draft, experimental analysis, and data analysis. QL: methodology, writing—review and editing, project administration, and funding acquisition. SZ: main idea, project administration. LL: experimental analysis. ZZ: data analysis. XL: experimental analysis and data analysis. All authors contributed to the article and approved the submitted version.

## REFERENCES

- Chen, C. M., Zhong, L. F., Wan, Z. F., Cheng, C. Y., Zhou, W., and Xu, X. (2022). Geochemical Characteristics of Cold-Seep Carbonates in Shenhu Area, South China Sea. *J. Oceanology Limnology*. 2022. doi:10.1007/s00343-021-1112-z
- Cong, X. R., Su, M., Wu, N. Y., Qiao, S. H., Sha, Z. B., Lu, H. L., et al. (2018). Contribution of Thermogenic Gases to Hydrate Accumulation under the marine Hydrocarbon-Rich Depression Setting. *Acta Geologica Sinica* 92 (1), 170–183.
- Deng, W., Liang, J. Q., Zhang, W., Kuang, Z. G., Tong, Z., and He, Y. L. (2021). Typical Characteristics of Fracture-Filling Hydrate-Charged Reservoirs Caused by Heterogeneous Fluid Flow in the Qiongdongnan Basin, Northern south China Sea. *Mar. Pet. Geology*. 124, 104810. doi:10.1016/j.marpetgeo.2020.104810
- Gan, J., Zhang, Y. Z., Liang, G., Yang, X. B., Yang, J. H., Li, X., et al. (2018). On Accumulation Process and Dynamic Mechanism of Natural Gas in the Deep Water Area of Central Canyon, Qiongdongnan Basin. *Acta Geologica Sinica* 92, 2359–2367. doi:10.1016/j.orggeochem.2018.09.002
- He, J. X., Su, P. B., Lu, Z. Q., Zhang, W., Liu, Z. J., and Li, X. T. (2015). Prediction of Gas Sources of Natural Gas Hydrate in the Qiongdongnan Basin, Northern South China Sea, and its Migration, Accumulation and Reservoir Formation Pattern. *Nat. Gas Industry* 35 (8), 19–29.
- Huang, B., Tian, H., Li, X., Wang, Z., and Xiao, X. (2016). Geochemistry, Origin and Accumulation of Natural Gases in the deepwater Area of the Qiongdongnan Basin, South China Sea. *Mar. Pet. Geology*. 72, 254–267. doi:10.1016/j.marpetgeo.2016.02.007
- Huang, H. T., Huang, B. J., Huang, Y. W., Li, X., and Tian, H. (2017). Condensate Origin and Hydrocarbon Accumulation Mechanism of the deepwater Giant Gas Field in Western South China Sea: A Case Study of Lingshui 17-2 Gas Field in Qiongdongnan Basin, South China Sea. *Pet. Exploration Development* 44 (3), 380–388. doi:10.1016/s1876-3804(17)30047-2
- Lai, H. F., Fang, Y. X., Kuang, Z. G., Ren, J. F., Liang, J. Q., LuWang, J. A. G. L., et al. (2021). Geochemistry, Origin and Accumulation of Natural Gas Hydrates in the Qiongdongnan Basin, South China Sea: Implications from Site GMGS5-W08. *Mar. Pet. Geology*. 123, 1–14. doi:10.1016/j.marpetgeo.2020.104774
- Li, X. S., Zhang, Y. Z., Yang, X. B., Xu, X. F., Zhang, J. X., and Man, X. (2017). New Understandings and Achievements of Natural Gas Exploration in Yinggehai-Qiongdongnan basin, South China Sea. *China Offshore Oil and Gas* 29 (6), 1–11.
- Liang, J. Q., Zhang, G. X., Lu, J. A., Su, P. B., Sha, Z. B., Gong, Y. H., et al. (2016). Accumulation Characteristics and Genetic Models of Natural Gas Hydrate Reservoirs in the NE Slope of the South China Sea (in Chinese). 36, 157–162.
- Liang, J., Zhang, W., Lu, J. A., Wei, J., Kuang, Z., and He, Y. (2019). Geological Occurrence and Accumulation Mechanism of Natural Gas Hydrates in the Eastern Qiongdongnan Basin of the South China Sea: Insights from Site GMGS5-W9-2018. *Mar. Geology*. 418, 106042. doi:10.1016/j.margeo.2019.106042

## FUNDING

The research is sponsored by the National Key Research and Development Plan of China (Grant Nos. 2016YFC0304000, and 2021YFC2800046), Special fund support of CNOOC, and National Natural Science Foundation of China (Grant Nos. U19B2005, and U20B6005).

## ACKNOWLEDGMENTS

The authors wish to thank all personnel of the drilling and logging technology trial of gas hydrate in the South China Sea in 2019 and 2021 led by CNOOC, for their field assistance and stimulating insights. Special thanks should be given to two reviewers, who have improved the manuscript thoroughly, and significantly.

- Milkov, A. V., and Etiope, G. (2018). Revised genetic diagrams for natural gases based on global dataset of b20,000 samples. *Org. Geochem*. 125, 109–120. doi:10.1016/j.orggeochem.2018.09.002
- Paganoni, M., King, J. J., Foschi, M., Mellor-Jones, K., and Cartwright, J. A. (2019). A Natural Gas Hydrate System on the Exmouth Plateau (NW Shelf of Australia) Sourced by Thermogenic Hydrocarbon Leakage. *Mar. Pet. Geology*. 99, 370–392. doi:10.1016/j.marpetgeo.2018.10.029
- Song, R. Y., Chen, K., Li, A. Q., Mao, H., and Liu, Y. Z. (2021). Representation of Gas Hydrate Fracture Migration System by Seismic. *Pet. Geology. Exp.* 43 (1), 136–143. doi:10.11781/sysydz202101136
- Wan, Z.-F., Zhang, W., Ma, C., Liang, J.-Q., Li, A., Meng, D.-J., et al. (2022). Dissociation of Gas Hydrates by Hydrocarbon Migration and Accumulation-Derived Slope Failures: An Example from the south china Sea. *Geosci. Front.* 13 (2), 101345. doi:10.1016/j.gsf.2021.101345
- Wan, Z., Chen, C., Liang, J., Zhang, W., Huang, W., and Su, P. (2020). Hydrochemical Characteristics and Evolution Mode of Cold Seeps in the Qiongdongnan Basin, South China Sea. *Geofluids* 2020 (6), 1–16. doi:10.1155/2020/4578967
- Wan, Z., Xu, X., Wang, X., Xia, B., and Sun, Y. (2017). Geothermal Analysis of Boreholes in the Shenhu Gas Hydrate Drilling Area, Northern South China Sea: Influence of Mud Diapirs on Hydrate Occurrence. *J. Pet. Sci. Eng.* 158, 424–432. doi:10.1016/j.petrol.2017.08.053
- Wan, Z., Zhang, J., Lin, G., Zhong, S., Li, Q., Wei, J., et al. (2021). Formation Mechanism of Mud Volcanoes/Mud Diapirs Based on Physical Simulation. *Geofluids* 2021, 1–16. doi:10.1155/2021/5531957
- Wang, J., Wu, S., Kong, X., Ma, B., Li, W., Wang, D., et al. (2018). Subsurface Fluid Flow at an Active Cold Seep Area in the Qiongdongnan Basin, Northern South China Sea. *J. Asian Earth Sci.* 168, 17–26. doi:10.1016/j.jseas.2018.06.001
- Wang, Z., Sun, Z., Zhu, J., Guo, M., and Jiang, R. (2015). Natural Gas Geological Characteristics and Great Discovery of Large Gas fields in Deep-Water Area of the Western South China Sea. *Nat. Gas Industry B* 2 (6), 489–498. doi:10.1016/j.ngb.2016.03.001
- Wei, J. G., Li, J. W., Wu, T. T., Zhang, W., Li, J. T., Wang, J. L., et al. (2020). Geologically Controlled Intermittent Gas Eruption and its Impact on Bottom Water Temperature and Chemosynthetic Communities—A Case Study in the “HaiMa” Cold Seeps, South China Sea. *Geol. J.* 50, 1–13. doi:10.1002/gj.3780
- Wei, J., Liang, J., Lu, J., Zhang, W., and He, Y. (2019). Characteristics and Dynamics of Gas Hydrate Systems in the Northwestern South China Sea - Results of the Fifth Gas Hydrate Drilling Expedition. *Mar. Pet. Geology*. 110, 287–298. doi:10.1016/j.marpetgeo.2019.07.028
- Xu, X. D., Zhang, Y. Z., Liang, G., Xiong, X. F., Li, X., Guo, X. X., et al. (2016). Hydrocarbon Source Condition and Accumulation Mechanism of Natural Gas in deepwater Area of Qiongdongnan Basin, Northern South China Sea. *Nat. Gas Geosci.* 27 (11), 1985–1992.
- Yang, L., Liu, B., Xu, M., Liu, S., Guan, Y., and Gu, Y. (2018). Characteristics of Active Cold Seepages in Qiongdongnan Sea Area of the Northern South China Sea. *Acta Geophysica Sinica* 61 (7), 2905–2914. doi:10.6038/cjg2018L0374
- Ye, J., Wei, J., Liang, J., Lu, J., Lu, H., and Zhang, W. (2019). Complex Gas Hydrate System in a Gas Chimney, South China Sea. *Mar. Pet. Geology*. 104, 29–39. doi:10.1016/j.marpetgeo.2019.03.023

- Zhang, G. C., Zeng, Q. B., Su, L., Yang, H. Z., Chen, Y., Yang, D. S., et al. (2016). Accumulation Mechanism of LS17-2 Deep Water Gaint Gas Field in Qiongdongnan Basin. *Acta Pet. Sin.* 37 (S1), 34–46.
- Zhang, K., Song, H., Wang, H., Tao, J., Guan, Y., Gong, Y., et al. (2020). A Preliminary Study on the Active Cold Seeps Flow Field in the Qiongdongnan Sea Area, the Northern South China Sea. *Chin. Sci. Bull.* 65, 1130–1140. doi:10.1360/tb-2019-0582
- Zhang, W., Liang, J., Liang, Q., Wei, J., Wan, Z., Feng, J., et al. (2021). Gas Hydrate Accumulation and Occurrence Associated with Cold Seep Systems in the Northern South China Sea: An Overview. *Geofluids* 2021, 1–24. doi:10.1155/2021/5571150
- Zhang, W., Liang, J. Q., Wei, J. G., Lu, J. A., Su, P. B., Lin, L., et al. (2019a). Geological and Geophysical Features of and Controls on Occurrence and Accumulation of Gas Hydrates in the First Offshore Gas-Hydrate Production Test Region in the Shenhu Area, Northern South China Sea. *Mar. Pet. Geology*. 114, 104191. doi:10.1016/j.marpetgeo.2019.104191
- Zhang, W., Liang, J., Su, P., Wei, J., Gong, Y., Lin, L., et al. (2019b). Distribution and Characteristics of Mud Diapirs, Gas Chimneys, and Bottom Simulating Reflectors Associated with Hydrocarbon Migration and Gas Hydrate Accumulation in the Qiongdongnan Basin , Northern Slope of the South China Sea. *Geol. J.* 54, 3556–3573. doi:10.1002/gj.3351
- Zhang, W., Liang, J., Wan, Z., Su, P., Huang, W., Wang, L., et al. (2020a). Dynamic Accumulation of Gas Hydrates Associated with the Channel-Levee System in the Shenhu Area, Northern South China Sea. *Mar. Pet. Geology*. 117, 104354. doi:10.1016/j.marpetgeo.2020.104354
- Zhang, W., Liang, J., Yang, X., Su, P., and Wan, Z. (2020b). The Formation Mechanism of Mud Diapirs and Gas Chimneys and Their Relationship with Natural Gas Hydrates: Insights from the Deep-Water Area of Qiongdongnan Basin, Northern South China Sea. *Int. Geology. Rev.* 62, 789–810. doi:10.1080/00206814.2018.1491014
- Zhang, Y. Z., Gan, J., Xu, X. D., Liang, G., and Li, X. (2019). The Source and Natural Gas Lateral Migration Accumulation Model of Y 8-1 Gas Bearing Structure, East Deep Water in the Qiongdongnan Basin. *Earth Sci.* 44 (08), 2609–2618.
- Zhu, W., Huang, B., Mi, L., Wilkins, R. W. T., Fu, N., and Xiao, X. (2009). Geochemistry, Origin, and Deep-Water Exploration Potential of Natural Gases in the Pearl River Mouth and Qiongdongnan Basins, South China Sea. *Bulletin* 93, 741–761. doi:10.1306/02170908099
- Zuo, Q. M., Zhang, D. J., Wang, Y. H., Li, W., Chen, Y., He, X. H., et al. (2016). Sedimentary Characteristics and Exploration Potential of Neogene Submarine Fan in the deepwater Area of the Qiongdongnan Basin[J]. *Acta Oceanologica Sinica* 38 (11), 105–116.
- Conflict of Interest:** Author QF was employed by the company CNOOC Research Institute, Beijing, China.
- The remaining authors declare that the research was conducted in the absence of any commercial or financial relationships that could be construed as a potential conflict of interest.
- Publisher's Note:** All claims expressed in this article are solely those of the authors and do not necessarily represent those of their affiliated organizations, or those of the publisher, the editors, and the reviewers. Any product that may be evaluated in this article, or any claim that may be made by its manufacturer, is not guaranteed or endorsed by the publisher.

Copyright © 2022 Fan, Li, Zhou, Li, Zhu and Lv. This is an open-access article distributed under the terms of the Creative Commons Attribution License (CC BY). The use, distribution or reproduction in other forums is permitted, provided the original author(s) and the copyright owner(s) are credited and that the original publication in this journal is cited, in accordance with accepted academic practice. No use, distribution or reproduction is permitted which does not comply with these terms.